Available online at www.sciencedirect.com
ScienceDirect
Ceramics International 37 (2011) 943–949
CERAMICS INTERNATIONAL
www.elsevier.com/locate/ceramint

Fabrication and properties of $CaZr_{0.9}In_{0.1}O_{3-\delta}$ prepared by an auto-ignition combustion process

Jingchao Zhang, Zhaoyin Wen *, Jinduo Han, Yu Liu, Shufeng Song, Ting-lian Wen

CAS Key Laboratory of Energy Conversion Materials, Shanghai Institute of Ceramics, Chinese Academy of Sciences, 1295 DingXi Road, Shanghai 200050, PR China

Received 29 July 2010; received in revised form 6 September 2010; accepted 30 October 2010
Available online 1 December 2010

Abstract

One of the major challenges in developing proton conducting $CaZr_{0.9}In_{0.1}O_{3-\delta}$ is to achieve a high densification at low sintering temperature. In this work, an auto-ignition combustion process was first used to synthesize $CaZr_{0.9}In_{0.1}O_{3-\delta}$ powders aiming to improve its sinterability. The products were characterized by X-ray diffraction (XRD), scanning electron microscopy (SEM), and dilatometry measurement. The results indicate that a calcination temperature of 1000 °C is sufficient to form the $CaZr_{0.9}In_{0.1}O_{3-\delta}$ phase. The as-obtained powders are fine, homogeneous and well crystallized, which strongly improves the sintering properties. Dense $CaZr_{0.9}In_{0.1}O_{3-\delta}$ ceramics with uniform grain size were obtained by sintering at 1350 °C, which is much lower than that required for the conventional solid state reaction method. In addition, the electrical properties of $CaZr_{0.9}In_{0.1}O_{3-\delta}$ ceramics were studied by electrochemical impedance spectroscopy.

Keywords: A. Powders: chemical preparation; A. Sintering; C. Impedance; D. Perovskites

1. Introduction

Trivalent-doped $CaZrO_3$ (e.g. In^{3+}, Y^{3+}, Gd^{3+}) conducts protons in humid or hydrogen-containing atmospheres [1–3], which, along with its excellent chemical and mechanical stability, make it a prime candidate for hydrogen sensing applications in liquid aluminum and copper. However, like other zirconates, these materials need a high sintering temperature and long holding time to achieve full density because of their high refractory nature [4]. Not only are these conditions energy consuming, they also bring about detrimental effect such as abnormal grain growth [5] and thereby lead to undesirable electrical and mechanical performances.

Wet chemical routes like sol–gel [6] and co-precipitation can improve ion homogeneity and reduce the temperatures required for phase formation [7]. These methods also help to produce high surface active powders that sinter better and thus obtain higher density ceramics [8]. Therefore, co-precipitation for the synthesis of In-doped $CaZrO_3$ has been investigated [9]. It could improve the agglomerate size by addition of PEG and ball milling for 2 days. However, no sintering properties were presented. In addition, Zhou and Ahmad [3] synthesized In-doped $CaZrO_3$ using a sol–gel method. The sintering temperature could be lowered to 1500 °C, although high porosity was still noticed.

The glycine–nitrate combustion has proved to be an effective technique for the preparation of nanocrystalline multi-component metal oxides [10]. It has the advantages of applying inexpensive raw materials, maintaining a relatively simple and fast preparation process, and achieving fine powders with high homogeneity [11]. To the best of our knowledge, this technique has not been reported for the preparation of $CaZr_{0.9}In_{0.1}O_{3-\delta}$. Hence, this work was initiated to synthesize the $CaZr_{0.9}In_{0.1}O_{3-\delta}$ applying the glycine–nitrate combustion process, with the principal objective of lowering its densification temperature. The sintering behavior of the as-prepared powders was compared with that by the conventional solid state reaction method. Moreover, the electrical properties of $CaZr_{0.9}In_{0.1}O_{3-\delta}$ ceramics were studied by the electrochemical impedance spectroscopy.

* Corresponding author. Tel.: +86 21 52411704; fax: +86 21 52413903.
E-mail address: zywen@mail.sic.ac.cn (Z. Wen).

0272-8842/$36.00
doi:10.1016/j.ceramint.2010.10.035

2. Experimental

2.1. Sample preparation

A possible combustion reaction between the nitrates and glycine can be represented as [12,13]:

$$Ca(NO_3)_2(aq) + 0.9Zr(NO_3)_4(aq) + 0.1In(NO_3)_3(aq) + 3.28NH_2CH_2COOH(aq) \rightarrow CaZr_{0.9}In_{0.1}O_{3-\delta}(s) + 4.59N_2(g) + 6.56CO_2(g) + 8.2H_2O(g)$$

Here, (aq), (s) and (g) means the liquid, solid and gas state, respectively. According to Mokkelbost et al. [14], a more violent reaction, where burning took place, was observed for the near stoichiometric and the fuel excess samples compared to the fuel deficiency sample. They also revealed that the near stoichiometric glycine/nitrate ratio is the optimal synthesis condition. Thus, for the present work a near stoichiometric glycine/nitrate ions ratio of 0.61 was used.

Aqueous solution containing ions of Ca, Zr and In were prepared by dissolving stoichiometric amount of $Ca(NO_3)_2{\cdot}4H_2O$, $Zr(NO_3)_4{\cdot}5H_2O$, and $In(NO_3)_3{\cdot}4.5H_2O$ powders (A.R.) in distilled water. Then the solution was slowly dropped into a glycine solution. The resulting mixture was stirred and heated at 70 °C until a transparent sol was obtained. The precursor formed by drying the transparent sol in an electric oven was then heated on a hot plate at about 147 °C in air, where ignition took place. Fig. 1 shows the flames produced during the combustion reaction. The spontaneous combustion went on vigorously for about 12 s, resulting in a porous, foamy and fragile material. The as-burnt powders were further calcined between 800 and 1100 °C for 5 h in air to remove the carbonaceous residues and to form a well crystalline structure. The products were denoted as GCP samples. To study the sintering behavior of the nanoparticles made by the combustion process, pellets were obtained by isostatically pressing the as-synthesized powders at 250 MPa and then sintering in air in the temperature range of 1350–1550 °C for 10 h.

Fig. 1. Flames produced during the combustion reaction.

For comparison, $CaZr_{0.9}In_{0.1}O_{3-\delta}$ was also prepared by the conventional solid state reaction method [15]. Stoichiometric amounts of $CaCO_3$ (A.R.), ZrO_2 (A.R.) and In_2O_3 (99.99%) were ball milled using ethanol as the medium for 10 h. The slurry yielded was dried and then calcined at 1000–1300 °C for 10 h. The products were marked SSR samples.

2.2. Characterization techniques

The phase evolution of powders was examined by X-ray diffraction analysis (Rigku RAD-C, 12 KW) at room temperature using Cu Kα radiation in the 2θ range from 5° to 80°. The average crystallite size D was estimated according to the Scherrer equation:

$$D = \frac{0.9\lambda}{\beta\cos\theta} \quad (2)$$

where λ is the X-ray wavelength (0.154056 nm), θ is the diffraction angle of the (1 2 1) peak, and β is the full width at half maximum (FWHM) of the (1 2 1) peak (in radian).The morphological features of powders were obtained on a field-emission scanning electron microscope (JEOL, JSM-6700F). Dilatometry (Netzsch, DIL 402C) on green body cylinders was performed in air with a heating rate of 5 °C min^{-1} up to 1350 °C. And the green body cylinders with size of Φ5 mm × 16 mm were made under 2 MPa pressure using the GCP powders and the SSR powders [16], respectively. Microstructures of the sintered ceramics and the Pt electrode were observed by the electron microscope (JEOL, JXA-8100).

The bulk density of the sintered ceramics was measured by the Archimedes method in ethanol. The theoretical density of the sinters was calculated based on crystal structure, mass and lattice parameter [17]. The relative density was derived from a ratio of bulk density to theoretical.

2.3. Electrical measurements

The sintered pellets were polished and then cleaned with ethanol in an ultrasonic cleaner. Pt electrodes were formed by painting the planar faces of the pellets with platinum paste and then firing at 800 °C for 1 h. Micrographs of the surface and cross section of the Pt electrode are shown in Fig. 2. It can be observed that the Pt electrode is porous and exhibits good adhesion to $CaZr_{0.9}In_{0.1}O_{3-\delta}$ ceramics.

Conductivity was measured from 400 to 800 °C in air by an AC method using a Solartron 1260 frequency response analyzer coupled with a 1287 electrochemical interface controlled by the electrochemical impedance software Zplot over the frequency range 10^{-2} to 3×10^6 Hz.

3. Results and discussion

3.1. Powder characteristics

Fig. 3 shows the X-ray diffraction patterns of the as-burnt powders and the powders derived from GCP and SSR method,

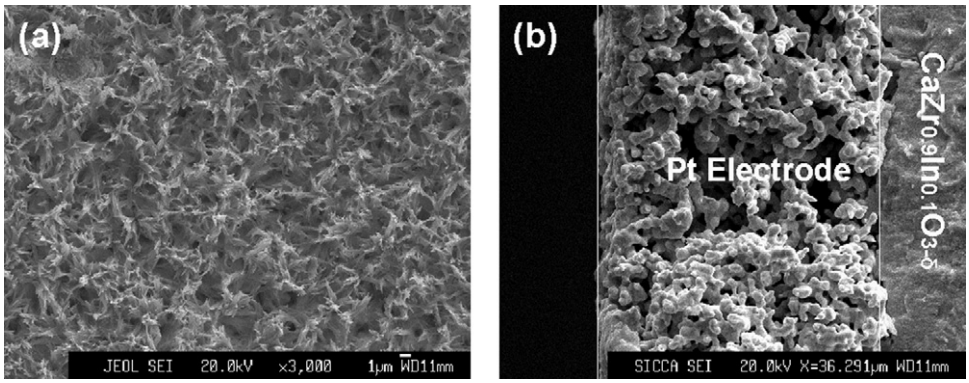

Fig. 2. Micrographs of the Pt electrode: (a) surface and (b) cross section.

respectively. According to Fig. 3, the as-burnt powders mainly consist of the $CaZr_{0.9}In_{0.1}O_{3-\delta}$ phase. Small diffraction line corresponding to an impurity phase can be assigned to $Ca_{0.15}Zr_{0.85}O_{1.85}$, although stoichiometric solution was used. Upon further thermal treatment at 1000 °C, the $Ca_{0.15}Zr_{0.85}O_{1.85}$ diffraction line decreases remarkably and only weak traces of it remain. The result is in good agreement with the XRD pattern of the doped $CaZrO_3$ reported in the literature [18]. Although an impurity phase is present, their very low content should not affect the transport properties obviously, as has been demonstrated in the literature [19]. While the powders calcined at 1000 °C by SSR method display lines due to the ZrO_2 phase.

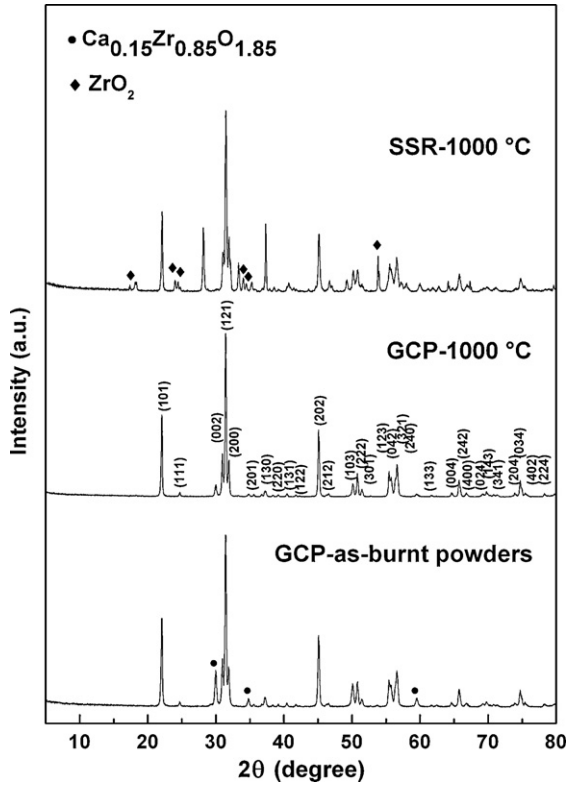

Fig. 3. XRD patterns of the as-burnt powders and $CaZr_{0.9}In_{0.1}O_{3-\delta}$ powders calcined at 1000 °C by the glycine–nitrate combustion process and solid state reaction method.

The morphology of the as-synthesized powders made by SSR and GCP method is presented by SEM micrographs in Fig. 4. As seen, the particles synthesized by GCP method are smaller and more homogeneous than the SSR powders. In fact, the crystallite size of GCP powders calculated from XRD data by the Scherrer equation for the representative diffraction line (1 2 1) was 39 nm. The small particle size synthesized through the glycine–nitrate combustion process can be accounted for bearing in mind the gases evolved during the combustion. The gas evolution spreads out of the reaction mass separating the particles, and also can help to dissipate the heat developed during the burning and hence, inhibiting the sintering of the particles. On the contrary, the particle size distribution of the SSR powders appears not uniform with some large particles.

3.2. Densification and microstructure

Fig. 5 compares the thermal shrinkage curve of $CaZr_{0.9}In_{0.1}O_{3-\delta}$ prepared by the glycine–nitrate combustion process with that prepared by the conventional solid state reaction method. The onset of sintering occurs at ~1010 °C for the glycine–nitrate combustion process, approximately 100 °C lower than the SSR sample. Furthermore, as the temperature reaches 1350 °C, the total shrinkage is about 14.4% for the glycine–nitrate combustion powders, which is more than seven times than the solid state reaction method (2.1%). The above results also indicate that $CaZr_{0.9}In_{0.1}O_{3-\delta}$ from the glycine–nitrate combustion process shows much higher density than SSR samples.

A relative density of 97.9% of the theoretical density was obtained for the $CaZr_{0.9}In_{0.1}O_{3-\delta}$ ceramics by the glycine–nitrate combustion process when the pellets were sintered at 1350 °C, which is about 250 °C lower than the earlier report by Kurita et al. [20]. Furthermore, in the study of Le et al. [21], 92% of the theoretical was obtained in $CaZr_{0.9}In_{0.1}O_{3-\delta}$ ceramics after sintering at 1550 °C using a co-precipitation technique. This difference in the densification behavior probably results from powder specificities like grain size, grain size distribution, grain morphology and grain agglomeration state.

Micrographs of the fractured surfaces of $CaZr_{0.9}In_{0.1}O_{3-\delta}$ ceramics sintered at 1350 and 1400 °C, respectively, verified

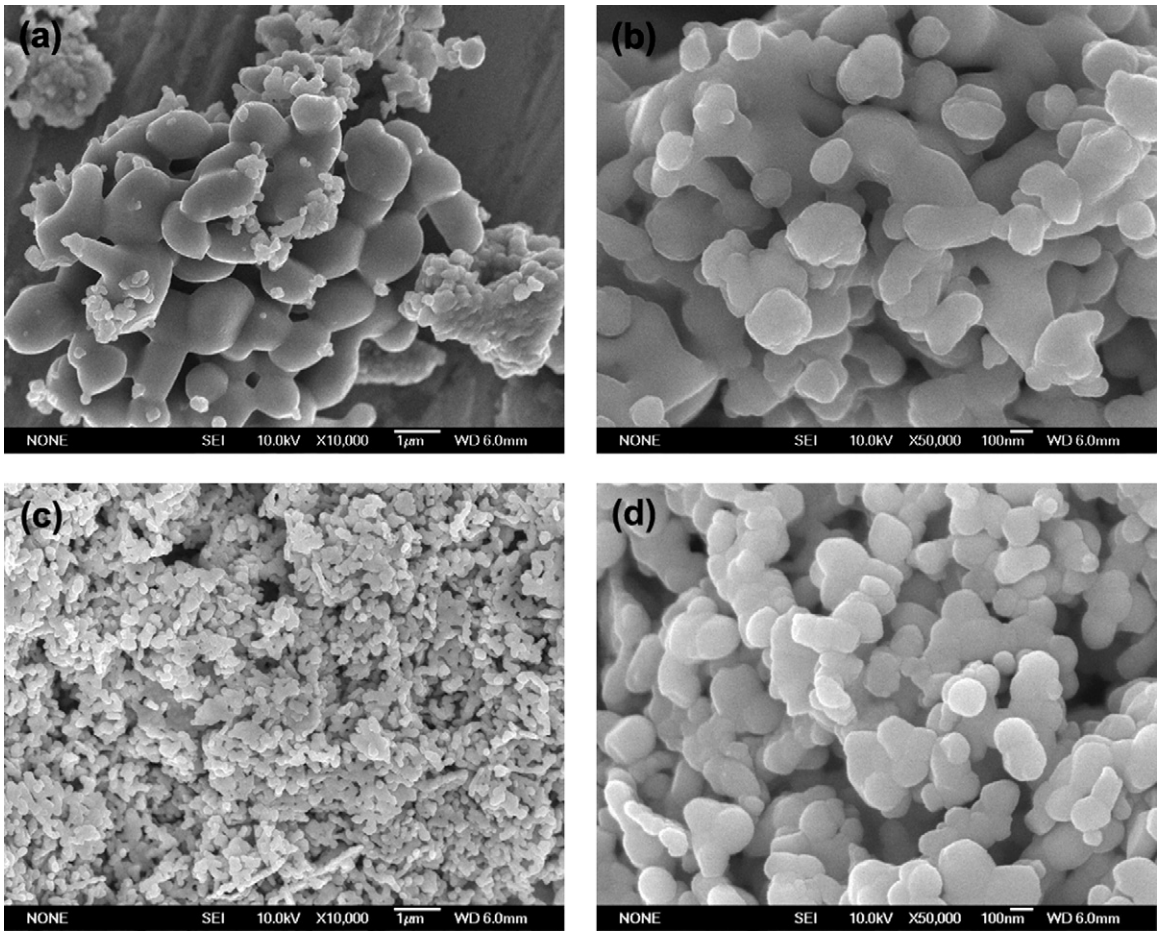

Fig. 4. SEM micrographs of $CaZr_{0.9}In_{0.1}O_{3-\delta}$ powders calcined at 1000 °C: (a and b) solid state reaction and (c and d) glycine–nitrate combustion process.

the results of density measurement, as shown in Fig. 6. It can be seen that the sample sintered at 1350 °C exhibits small and uniform grain size with few closed pores. As the sintering temperature increases, the grain size increases and the porosity decreases. However, the grains still remain relatively small (<3 μm) and in homogeneous distribution.

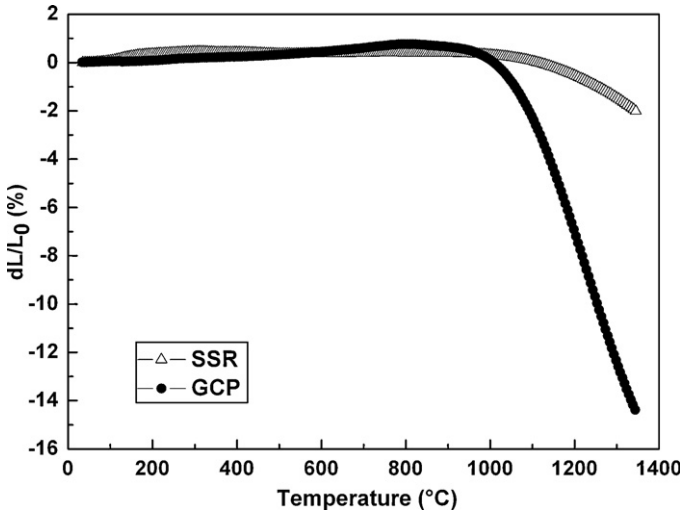

Fig. 5. Thermal shrinkage behaviors of $CaZr_{0.9}In_{0.1}O_{3-\delta}$ made by solid state reaction and the glycine–nitrate combustion process.

It can be concluded that $CaZr_{0.9}In_{0.1}O_{3-\delta}$ ceramics with enhanced densification and microstructure are obtained using the powders derived from the glycine–nitrate combustion process. The ultra fine nature of $CaZr_{0.9}In_{0.1}O_{3-\delta}$ nanopowder synthesized in the present study is responsible for the higher sinterability and higher densification. The high surface area of the particles provides a substantial driving force for sintering, which would reduce the sintering activation energy. Lowering sintering temperature will then become feasible [22–24].

3.3. Impedance spectrum

The effect of the sintering temperature of the samples on the electrical properties was determined with electrochemical impedance spectroscopy. Representative impedance spectra measured at 600, 700 and 800 °C in air are shown in Fig. 7 for the $CaZr_{0.9}In_{0.1}O_{3-\delta}$ ceramics sintered at different temperatures. At 600, 700 and 800 °C, the first semicircle has disappeared due to the low bulk capacity [25] and only the second semicircle and the tail are present. According to the commonly accepted "brick layer" model, the first (high frequency) semicircle corresponds to the bulk response, and the second semicircle is attributed to the grain-boundary resistance. The tail is related to the processes occurring at the electrodes

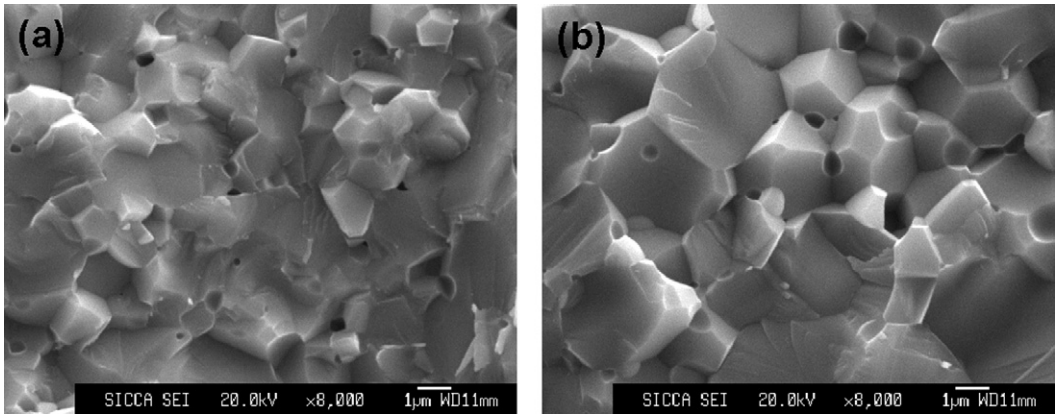

Fig. 6. Microstructure of fractured $CaZr_{0.9}In_{0.1}O_{3-\delta}$ ceramics sintered at different temperatures: (a) 1350 °C and (b) 1400 °C.

[26]. The bulk and total resistances of the sample can be determined from the left side intercept and the right side intercept by fitting the second semicircle with the real axis. And the grain-boundary resistance is equal to the difference between the right side intercept and the left one on the real axis. As is seen from Fig. 7, the arcs shift towards higher frequencies with increasing testing temperature, which indicates that the resistances decrease. It can also be deduced that both the grain-boundary resistance and the total resistance of $CaZr_{0.9}In_{0.1}O_{3-\delta}$ ceramics decrease with sintering temperature, and reach their minimum at 1500 °C. Further increase of sintering temperature might lead to the increase of resistance. This can be explained by the relationship of sintering temperature with grain size, density and phase homogeneity. As is referred by Wang et al. [27], excessively high sintering temperature and long duration will result in abnormal grain growth, low density and inhomogeneity of $CaZr_{0.9}In_{0.1}O_{3-\delta}$ ceramics and thereby lead to poor performances [28].

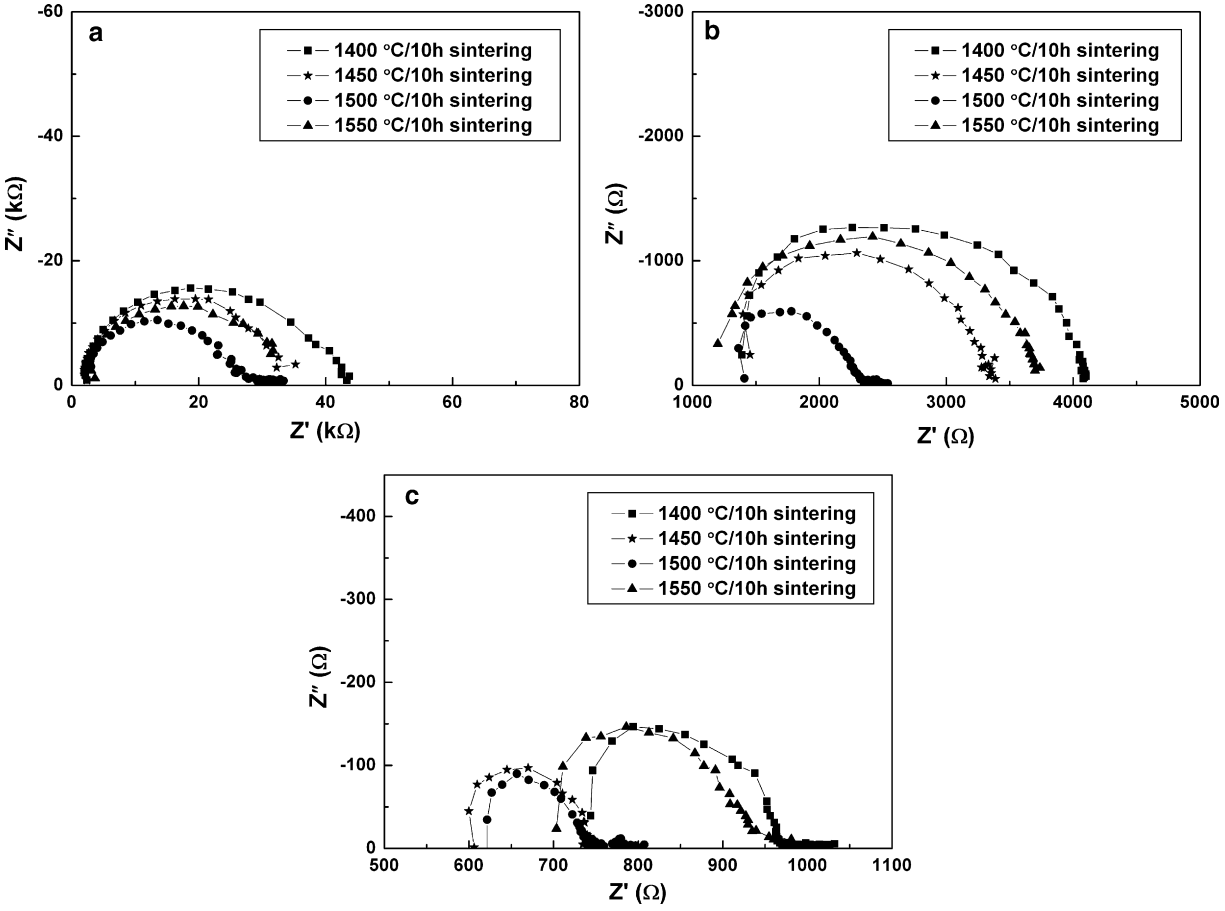

Fig. 7. Impedance spectra of $CaZr_{0.9}In_{0.1}O_{3-\delta}$ ceramics measured at (a) 600 °C; (b) 700 °C; (c) 800 °C in air.

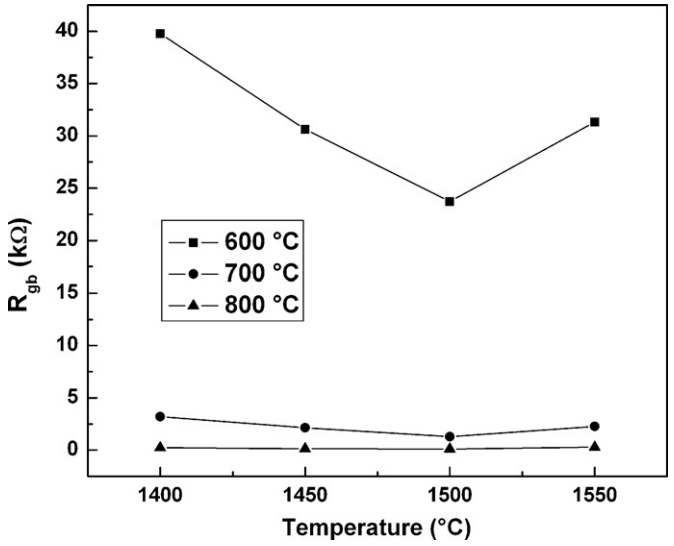

Fig. 8. Grain-boundary resistances of $CaZr_{0.9}In_{0.1}O_{3-\delta}$ ceramics sintered at different temperatures.

Fig. 8 gives the grain-boundary resistances of $CaZr_{0.9}In_{0.1}O_{3-\delta}$ ceramics sintered between 1400 and 1550 °C. As can be seen, the increase of the testing temperature results in a significant decline of the grain-boundary resistance. Meanwhile, the ceramics sintered at 1500 °C always shows the lowest grain-boundary resistance in the testing temperature range of 600–800 °C. At 700 °C, the total resistance of $CaZr_{0.9}In_{0.1}O_{3-\delta}$ ceramics sintered at 1500 °C is $2.29 \times 10^3\ \Omega$, which is close to but lower than $2.90 \times 10^3\ \Omega$ reported in the literature [3].

The conductivities can be calculated from the respective *R*-values using the bulk dimensions of the sample (diameter *d* and surface *S*) [29]:

$$\sigma = \frac{d}{R \times S} \tag{3}$$

According to the above equation, it can be deduced that $CaZr_{0.9}In_{0.1}O_{3-\delta}$ ceramics sintered at the optimum sintering temperature of 1500 °C possesses an optimal conductivity as a result of achieving optimum values of density, grain size and phase homogeneity.

4. Conclusions

The glycine–nitrate combustion process has been proved to be effective for the synthesis of pure $CaZr_{0.9}In_{0.1}O_{3-\delta}$ powders with fine and homogeneous crystal structure at the temperature as low as 1000 °C. In comparison with the conventional solid state reaction method, the glycine–nitrate combustion process remarkably increases the sintering rate of $CaZr_{0.9}In_{0.1}O_{3-\delta}$. A relative density of 97.9% was obtained at 1350 °C, which is about 250 °C lower than the earlier report. The conductivity of $CaZr_{0.9}In_{0.1}O_{3-\delta}$ ceramics presents an optimal value when the sintering temperature is 1500 °C, which can be interpreted with the relationship of sintering temperature with grain size, density and phase homogeneity.

Acknowledgements

This work has been supported by Natural Science Foundation of China (NSFC, Project No. 50802108) and Science and Technology Commission of Shanghai Municipality No. 08DZ2210900. The authors would also like to thank Ms. Zhonghua Gu and Mr. Xiaohe Xu for their help with experiments.

References

[1] H. Iwahara, T. Yajima, T. Hibino, K. Ozaki, H. Suzuki, Protonic conduction in calcium, strontium and barium zirconates, Solid State Ionics 61 (1993) 65–69.
[2] G.C Mather, F.M. Figueiredo, J.R. Jurado, J.R. Frade, Synthesis and characterisation of cermet anodes for SOFCs with a proton-conducting ceramic phase, Solid State Ionics 162–163 (2003) 115–120.
[3] M.H. Zhou, A. Ahmad, Sol–gel processing of In-doped $CaZrO_3$ solid electrolyte and the impedimetric sensing characteristics of humidity and hydrogen, Sens. Actuators B 129 (2008) 285–291.
[4] Z.Z. Peng, R.S. Guo, Z.G. Yin, J. Li, Influence of ZnO on the properties of $SrZr_{0.9}Y_{0.1}O_{2.95}$ protonic conductor, J. Am. Ceram. Soc. 91 (2008) 1534–1538.
[5] T. Schober, H.G. Bohn, Water vapor solubility and electrochemical characterization of the high temperature proton conductor $BaZr_{0.9}Y_{0.1}O_{2.95}$, Solid State Ionics 127 (2000) 351–360.
[6] A. Sin, Yu. Dubitsky, A. Zaopo, A.S. Aricò, L. Gullo, D. La Rosa, S. Siracusano, V. Antonucci, C. Oliva, O. Ballabio, Preparation and sintering of $Ce_{1-x}Gd_xO_{2-x/2}$ nanopowders and their electrochemical and EPR characterization, Solid State Ionics 175 (2004) 361–366.
[7] I.E. Gonenli, A.C. Tas, Chemical synthesis of pure and Gd-doped $CaZrO_3$ powders, J. Eur. Ceram. Soc. 19 (1999) 2563–2567.
[8] C. Laberty-Robert, F. Ansart, S. Castillo, G. Richard, Synthesis of YSZ powders by the sol–gel method: surfactant effects on the morphology, Solid State Sci. 4 (2002) 1053–1059.
[9] V. Krishnan, J.W. Fergus, Effects of dispersant addition on the synthesis of indium-doped calcium zirconate by co-precipitation techniques, J. Mater. Sci. 42 (2007) 6117–6122.
[10] L. da Conceição, N.F.P. Ribeiro, J.G.M. Furtado, M.M.V.M. Souza, Effect of propellant on the combustion synthesized Sr-doped $LaMnO_3$ powders, Ceram. Int. 35 (2009) 1683–1687.
[11] N. Kikukawa, M. Takemori, Y. Nagano, M. Sugasawa, S. Kobayashi, Synthesis and magnetic properties of nanostructured spinel ferrites using a glycine–nitrate process, J. Magn. Magn. Mater. 284 (2004) 206–214.
[12] L.A. Chick, L.R. Pederson, G.D. Maupin, J.L. Bates, L.E. Thomas, G.J. Exarhos, Glycine–nitrate combustion synthesis of oxide ceramic powders, Mater. Lett. 10 (1–2) (1990) 6–12.
[13] C.C. Hwang, J.S. Tsai, T.H. Huang, C.H. Peng, S.Y. Chen, Combustion synthesis of Ni–Zn ferrite powder—influence of oxygen balance value, J. Solid State Chem. 178 (2005) 382–389.
[14] T. Mokkelbost, I. Kaus, T. Grande, M.A. Einarsrud, Combustion synthesis and characterization of nanocrystalline CeO_2-based powders, Chem. Mater. 16 (2004) 5489–5494.
[15] T. Omata, M. Takagi, S. Otsuka-Yao-Matsuo, O–H stretching vibrations proton conducting alkaline-earth zirconates, Solid State Ionics 168 (2004) 99–109.
[16] J.D. Han, Z.Y. Wen, J.C. Zhang, Z.H. Gu, X.H. Xu, Fabrication of dense $CaZr_{0.90}In_{0.10}O_{3-\delta}$ ceramics from the fine powders prepared by an optimized solid-state reaction method, Solid State Ionics 179 (2008) 1108–1111.
[17] N. Sammes, R. Phillips, A. Smirnova, Proton conductivity in stoichiometric and sub-stoichiometric yittrium doped $SrCeO_3$ ceramic electrolytes, J. Power Sources 134 (2) (2004) 153–159.
[18] H.W. Zhang, X.Y. Fu, S.Y. Niu, Q. Xin, Blue luminescence of nanocrystalline $CaZrO_3$: Tm phosphors synthesized by a modified Pechini sol–gel method, J. Lumin. 128 (2008) 1348–1352.

[19] Z.J. Li, R.Q. Liu, Y.H. Xie, S. Feng, J.D. Wang, A novel method for preparation of doped $Ba_3(Ca_{1.18}Nb_{1.82})O_{9-\delta}$: application to ammonia synthesis at atmospheric pressure, Solid State Ionics 176 (11–12) (2005) 1063–1066.
[20] N. Kurita, N. Fukatsu, K. Ito, T. Ohashi, Proton conduction domain of indium-doped calcium zirconate, J. Electrochem. Soc. 142 (1995) 1552–1559.
[21] J. Le, L.N. van Rij, R.C. van Landschoot, J. Schoonman, A wet-chemical method for the synthesis of In-doped $CaZrO_3$ ceramic powders, J. Eur. Ceram. Soc. 19 (1999) 2589–2591.
[22] J.R. Groza, Nanosintering, Nanostruct. Mater. 12 (1999) 987–992.
[23] M. Mazaheri, A.M. Zahedi, S.K. Sadrnezhaad, Two-step sintering of nanocrystalline ZnO compacts: effect of temperature on densification and grain growth, J. Am. Ceram. Soc. 91 (2008) 56–63.
[24] K. Maca, M. Trunec, P. Dobask, Bulk zirconia nanoceramics prepared by cold isostatic pressing and pressureless sintering, Rev. Adv. Mater. Sci. 10 (2005) 84–88.
[25] B. Groβ, St. Marion, R. Hempelmann, D. Grambole, F. Herrmann, Influence of microstructure on electrical properties in $BaZr_{0.5}In_{0.5}O_{3-\delta}$ proton conductor, Solid State Ionics 109 (1998) 13–23.
[26] H.G. Bohn, T. Schober, Electrical conductivity of the high-temperature proton conductor $BaZr_{0.9}Y_{0.1}O_{2.95}$, J. Am. Ceram. Soc. 83 (2000) 768–772.
[27] D. Wang, C.J. Shi, C.M. Liu, C.Z. Wang, Preparation and characterization of high temperature proton conductor tube $CaZr_{0.9}In_{0.1}O_{3-\alpha}$, Acta Metall. Sinica 44 (2008) 177–182.
[28] P. Babilo, S.M. Haile, Enhanced sintering of yttrium-doped barium zirconate by addition of ZnO, J. Am. Ceram. Soc. 88 (2005) 2362–2368.
[29] F.M.M. Snijkers, A. Buekenhoudt, J. Cooymans, J.J. Luyten, Proton conductivity and phase composition in $BaZr_{0.9}Y_{0.1}O_{3-\delta}$, Scripta Mater. 50 (5) (2004) 655–659.